Anal. Chem. **2003,** *75,* 2522−2527

Rapid Prototyping of 2D Structures with Feature Sizes Larger than 8 μm

Vincent Linder, Hongkai Wu,† Xingyu Jiang, and George M. Whitesides*

Department of Chemistry and Chemical Biology, Harvard University, 12 Oxford Street, Cambridge, Massuchusetts 02138

This paper extends rapid prototyping for several types of lithography to the 8−25-μm size range, using transparency photomasks prepared by photoplotting. It discusses the technical improvement in photomask quality achieved by photoplotting, compared to the currently used image setting, and demonstrates differences in the resolution that can be obtained with photomasks with features in the 8−100-μm size range. These high-resolution photomasks were used to microfabricate microelectrodes, microlenses, and stamps for microcontact printing, following methods described previously.

This paper compares the ability of two types of commercial, high-resolution printers to print transparency photomasks—masks consisting of printed opaque regions on a flexible, transparent, supporting polymer film—for use in soft lithography.[1−4] We demonstrate that a new type of printer, known as a "photoplotter", can generate structures with features as small as 8 μm; older procedures relying on image setting techniques were limited to features of ≥25 μm. The turnaround time for these high-resolution transparency photomasks is equivalent to that of image setting products, and they are therefore available commercially within ∼2 days for a price similar to those obtained by image setting. They offer a fast, low-cost (<$1/in.^{2}) route to photoresist patterns over areas as large as 500 in.^{2}. These patterns are characterized by an edge roughness of ∼1 μm. Using standard photolithographic processes or soft lithography,[1] feature sizes in the 8−25-μm range become readily available, based on these new masks. These sizes extend the utility of rapid prototyping for applications in microelectromechanical systems, microsensors, optical components, and microfluidic systems. The 8−25-μm range is also useful for work in cell biology.

We first demonstrated the use of transparency films as photomasks with ≥25-μm resolution using image setting.[5] This technique—a form of rapid prototyping—has become an important part of soft lithography.[1−4,6−13] By further miniaturizing a commercial transparency film onto a microfiche,[14] we achieved 10-μm resolution, with edge roughness of 1 μm. This multistep approach was, however, only applicable to small areas (∼3−4 in.^{2}), and the light absorbing part of the mask suffered from incomplete opacity due to the nature of the silver grain in the microfiche. Later we simplified this approach by starting the process with a pattern printed onto paper with a commercial office printer instead of a high-resolution transparency.[15] We obtained microfiche patterns with resolution similar to the ones created from high-resolution photomask transparencies.

Laser photoplotting and laser image setting are two similar, specialized forms of photography.[16] To create an image, a beam of light strikes the surface of a light-sensitive photographic film. Processing of the film reveals the recorded image. Photoplotters were specifically designed and built for high-accuracy, tight-tolerance engineering artwork. They contain higher precision optics than image setters, for better control of line-edge definition and width, and they employ finer stepper motors for higher resolution and more accurate placement of features. They therefore achieve better performance than image setters. State-of-the-art laser photoplotters have beam sizes (sometimes referred to as "final spot size") of less than 2 μm and resolutions of 20 000 dots/in. (dpi).[16] These photoplotters use photosensitive films having resolutions that match the technical capabilities of their optical systems. The photoplotter films rely on a photographic emulsion made of very fine, highly sensitive silver halide grain that can take advantage of the small size of the laser beam. By combining high dpi capability with high photographic film quality, photoplotters generate sharper, finer images than image setters.

* Corresponding author. Telephone: (617) 495−9430. Fax: (617) 495−9857. E-mail: gwhitesides@gmwgroup.harvard.edu.

† Present address: Department of Chemistry, Stanford University, Stanford, CA, 94305-5080.

(1) Xia, Y. N.; Whitesides, G. M. *Angew. Chem., Int. Ed. Engl.* **1998**, *37*, 550−575.
(2) Ng, J. M. K.; Gitlin, I.; Stroock, A. D.; Whitesides, G. M. *Electrophoresis* **2002**, *23*, 3461−3473.
(3) Michel, B.; Bernard, A.; Bietsch, A.; Delamarche, E.; Geissler, M.; Juncker, D.; Kind, H.; Renault, J. P.; Rothuizen, H.; Schmid, H.; Schmidt-Winkel, P.; Stutz, R.; Wolf, H. *Chimia* **2002**, *56*, 527−542.
(4) Ma, H.; Jen, A. K. Y.; Dalton, L. R. *Adv. Mater.* **2002**, *14*, 1339−1365.
(5) Qin, D.; Xia, Y. N.; Whitesides, G. M. *Adv. Mater.* **1996**, *8*, 917−919.
(6) Unger, M. A.; Chou, H. P.; Thorsen, T.; Scherer, A.; Quake, S. R. *Science* **2000**, *288*, 113−116.
(7) Lu, Y.; Yin, Y.; Gates, B.; Xia, Y. N. *Langmuir* **2001**, *17*, 6344−6350.
(8) Tien, J.; Nelson, C. M.; Chen, C. S. *Proc. Natl. Acad. Sci. U.S.A.* **3002**, *99*, 1758−1762.
(9) Childs, W. R.; Nuzzo, R. G. *J. Am. Chem. Soc.* **2002**, *124*, 13583−13596.
(10) Yousaf, M. N.; Houseman, B. T.; Mrksich, M. *Proc. Natl. Acad. Sci. U.S.A.* **2001**, *98*, 5992−5996.
(11) Linder, V.; Verpoorte, E.; Thormann, W.; de Rooij, N. F.; Sigrist, H. *Anal. Chem.* **2001**, *73*, 4181−4189.
(12) Seong, G. H.; Zhan, W.; Crooks, R. M. *Anal. Chem.* **2002**, *74*, 3372−3377.
(13) Liu, Y.; Fangguy, J. C.; Bledsoe, J. M.; Henry, C. S. *Anal. Chem.* **2000**, *72*, 5939−5944.
(14) Deng, T.; Tien, J.; Xu, B.; Whitesides, G. M. *Langmuir* **1999**, *15*, 6575−6581.
(15) Deng, T.; Wu, H.; Brittain, S. T.; Whitesides, G. M. *Anal. Chem.* **2000**, *72*, 3176−3180.
(16) Personal communication from R. Martino, CAD/Art Services, Inc., 2002.

10.1021/ac026441d CCC: $25.00
Published on Web 04/12/2003

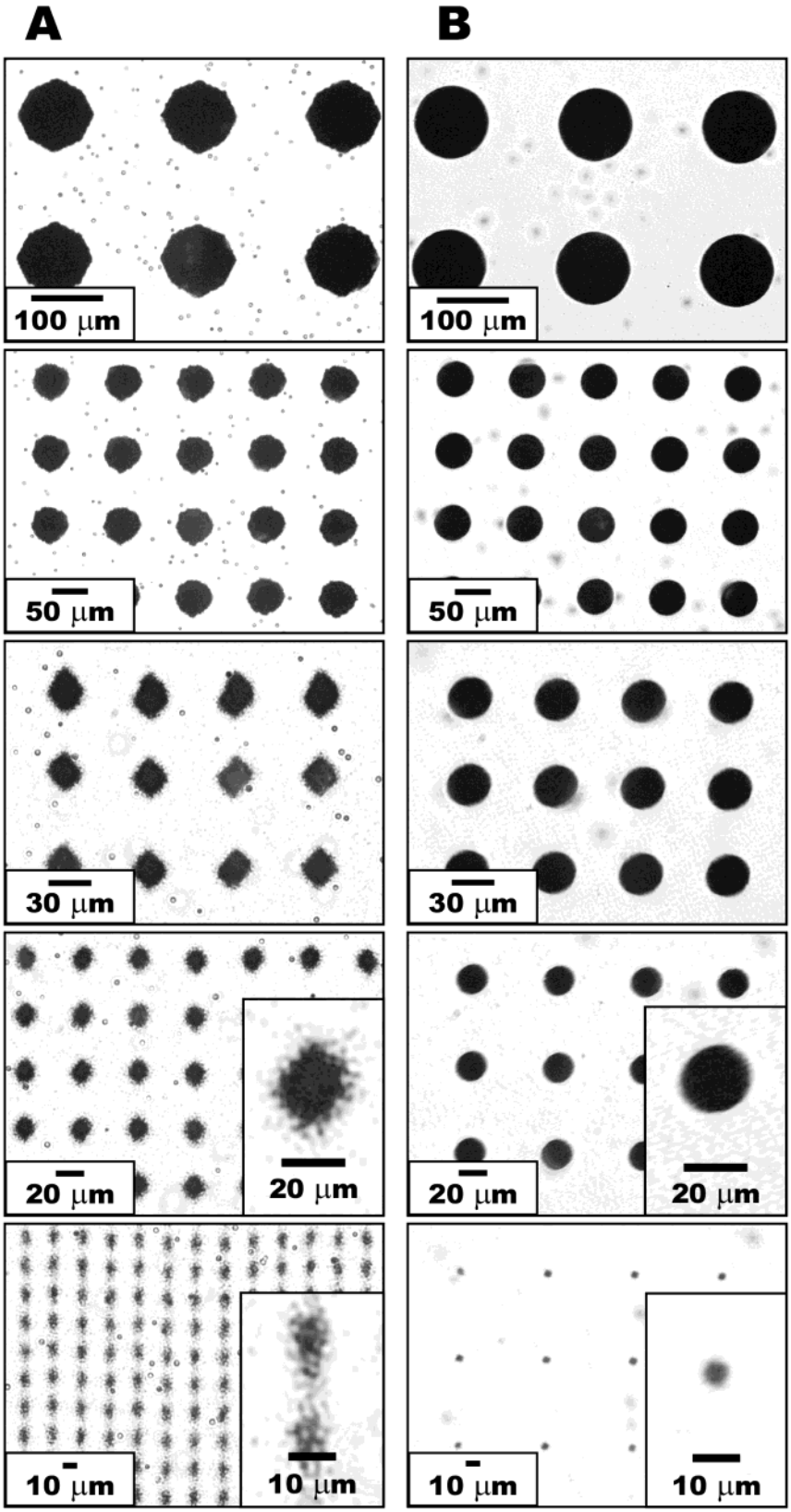

Figure 1. Optical microscopy pictures of photomasks generated by (A) image setting and (B) photoplotting. According to the layout drawn with CAD, the expected circle dimensions are 100, 50, 30, 20, and 10 μm, as indicated in the scale boxes.

This paper compares the resolution of simple features—lines, curves, and geometric shapes—on photomasks generated by commercial image setters and photoplotters. It demonstrates that photoplotters generate higher resolution masks than imagersetters and applies these photomasks (with photolithography) to prepare metallic microelectrodes and arrays of microlenses. By patterning negative photoresist, we also produced and used a stamp for microcontact printing. The use of photoplotting enables the

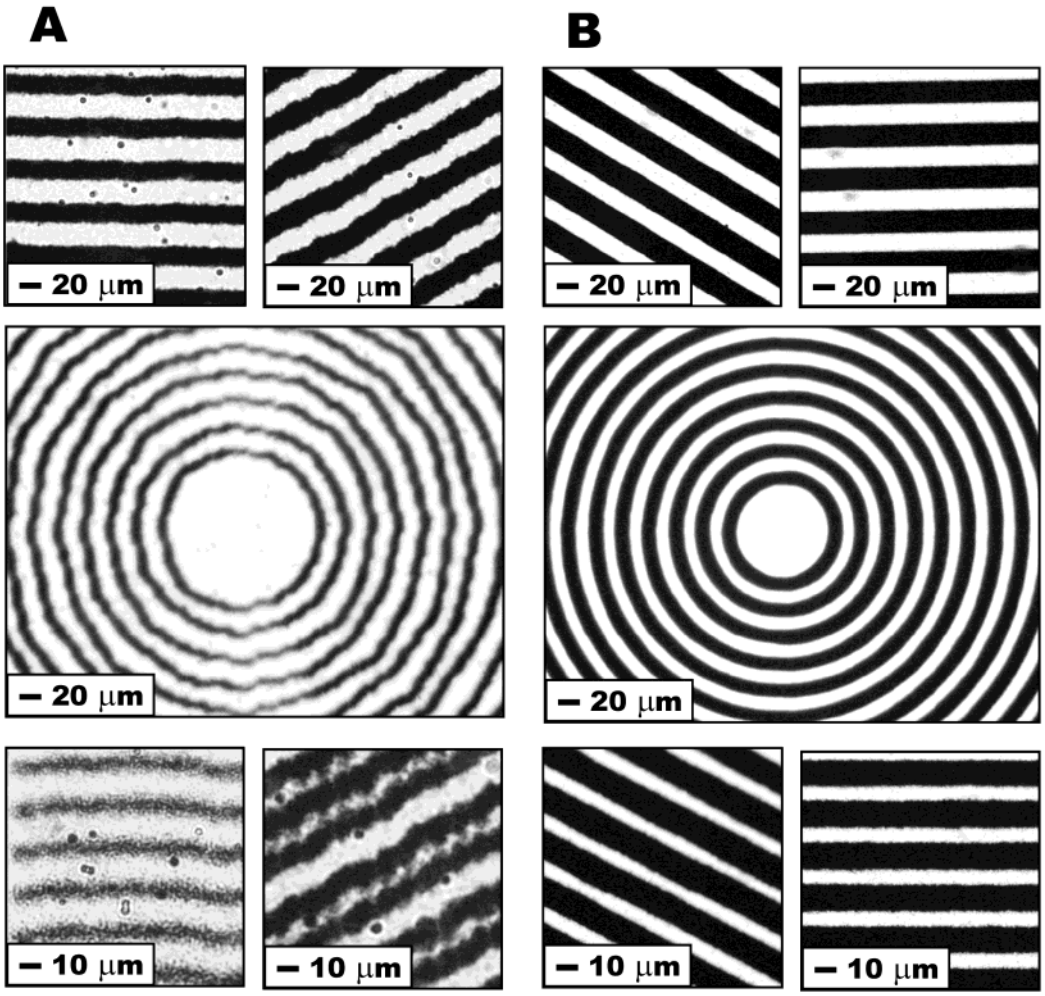

Figure 2. Optical microscopy pictures of photomasks processed by (A) image setting and (B) photoplotting. (Top) Horizontal and 30°-tilted 20-μm-wide lines; (middle) concentric circles, line width is 13 μm; (bottom) horizontal and 30°-tilted 10-μm-wide lines. Line and curve widths are given according to the original CAD layout.

preparation of photolithographic photomasks with high-quality structures in the sub-100 μm domain and features down to 8 μm. This extends the domain of application of rapid prototyping from ~25 to 8 μm line widths.

EXPERIMENTAL SECTION

Reagents and Materials. Image setting photomasks were purchased from PageWorks (Cambridge, MA; www.pageworks.com). Photoplotted photomasks were obtained from CAD/Art Services (Poway, CA; www.outputcity.com). Light transmission through the photomasks was measured using UV−visible spectroscopy (8453, Hewlett-Packard, Palo Alto, CA). Negative photoresist SU8-10 was purchased from Microchem (Newton, MA). Microposit 1818 and 1805 photoresists were bought from Shipley Co. Inc. (Marlborough, MA). Poly(dimethylsiloxane) Sylgard184 (PDMS) was ordered from Dow Corning (Midland, MI). Passage-12 primary bovine capillary endothelial (BCE) cells were suspended in Dulbecco's modification of Eagle's medium (DMEM, JRH Biosciences, Kansas City, MO) containing 10% (v/v) bovine calf serum (Invitrogen, Chicago, IL), 10 mM HEPES buffer ((*N*-(2-hydroxyethyl)piperazine-*N*′-(2-ethanesulfonic acid), Invitrogen) and glutamine−penicillin−streptomycin antibiotics (295 μg/mL, 100 units/mL and 100 μg/mL respectively, Invitrogen). Phosphate-buffered saline (PBS) was purchased from Invitrogen. Fibronectin was obtained from Sigma (St. Louis, MO). BCE cells were stained with phalloidin Alexa Fluor 488 (488-phalloidin, Molecular Probes, Eugene, OR) and mounted in 4′,6-diamidino-2-phenylindole (DAPI)-containing mounting media (Vectashield, Burlingame, CA). The (1-mercaptoundec-11-yl)hexa(ethylene glycol) molecule (HS-C_{11}-EG_6) was synthesized as described by Pale-Grosdemange et al.[17] and 1-octadecanethiol (HS-C_{18}) was purchased from Sigma.

Fabrication of Microlenses. Arrays of microlenses are the basis for microlens array photolithography, a method of making repetitive arrays of features with dimensions down to 0.5−1 μm.[18] The detailed procedure used to fabricate microlenses has been described earlier.[19] Briefly, an array of circular posts made of Shipley 1818 positive photoresist was generated by photolithography. The photoresist was then melted at 150 °C to turn the posts into lenses.

Fabrication of Gold Electrodes and Palladium Structures. The liftoff procedure has been described earlier.[20] Shipley 1805 photoresist was photolithographically patterned, and then a 1.5-

(17) Pale-Grosdemange, C.; Simon, E. S.; Prime, K. L.; Whitesides, G. M. *J. Am. Chem. Soc.* **1991**, *113*, 12−20.
(18) Wu, M. H.; Paul, K. E.; Yang, J.; Whitesides, G. M. *Appl. Phys. Lett.* **2002**, *80*, 3500−3502.
(19) Wu, H. K.; Odom, T. W.; Whitesides, G. M. *Anal. Chem.* **2002**, *74*, 3267−3273.

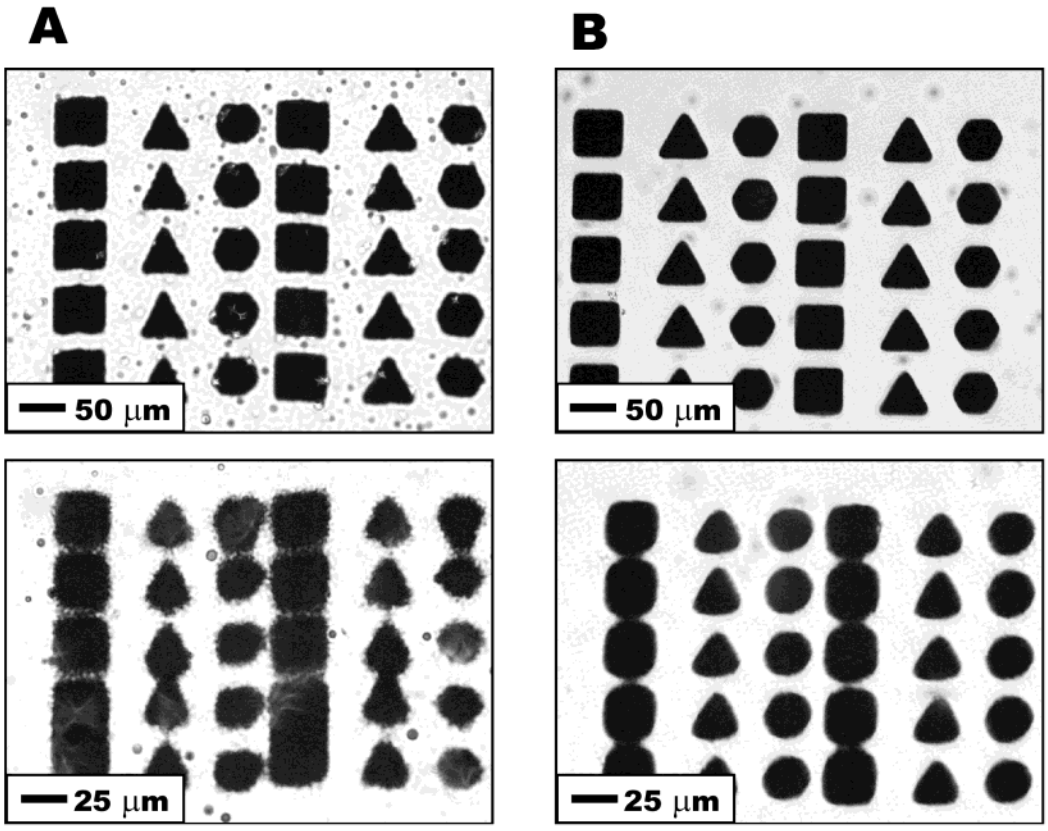

Figure 3. Optical microscopy pictures of polygon arrays printed on photomasks by (A) image setting and (B) photoplotting. Polygon dimensions are (top) 50 and (bottom) 25 μm.

nm adhesion layer of titanium and a 50-nm gold (or palladium) layer were evaporated on the substrate. Liftoff was carried out in ethanol.

BCE Cells on Patterned SAMs. The preparation of hydrophilic−hydrophobic patterns of thiols SAMs on gold substrates[21] by microcontact printing (μCP)[22] and the growth of cells on the hydrophobic adhesive areas[23] have been described earlier. Briefly, the pattern of the transparency mask was transferred by photolithography into an SU8-10 negative photoresist film, which was used as a casting template for a PDMS stamp. A pattern of HS-C_{11}-EG_6 and HS-C_{18} was generated on a gold-coated glass substrate by μCP using the elastomeric stamp. Patterned substrates were incubated for 1 h in a 5 μg/mL fibronectin solution in PBS, and a 2-mL suspension of BCE cells at 35 kcell/mL in DMEM was introduced on each 20 × 20 mm substrate. After 20 h, the cells were fixed, stained with 488-phalloidin and DAPI, and observed by fluorescence microscopy, as described previously.[24]

RESULTS AND DISCUSSION

Photomask Characterization. We have created simple patterns using CAD software, purchased the corresponding photomasks made by image setting and photoplotting from our suppliers, and compared the photomask resolution by optical microscopy. Figure 1 shows arrays of circles of diameters ranging from 100 to 10 μm. Circles processed by image setting are polygonal. At 30- and 20-μm diameters, circles appear diamond-shaped and the overall diameters of the shapes differ from the specifications by 10−20%. The 10-μm-diameter circles lost the transparent−opaque contrast between individual features. Circles processed by photoplotting are round, and their diameters match the specified value down to 20 μm. Circles drawn at 10 μm resulted in circles, but with a diameter of 7 μm. In Figure 2, we investigated the resolution of lines and curves. The 20-μm-wide lines obtained by image setting appear well resolved. They are certainly useful for applications where poor edge roughness is not critical. The line weight of the concentric curves is uneven: they show an ∼30% variation in width. These lines appear thinner than expected, as they are 9 μm wide, on average, instead of 13 μm. At 10 μm, lines become ill-defined and the transparent−opaque contrast of the photomask becomes insufficient for photolithography. The lines and curves produced by photoplotting are well-defined, and line weight appears as expected down to 13 μm. Straight lines drawn at 10 μm have a 30% increase in width but less than 1-μm edge roughness. On photoplotted photomasks, lines tilted with a 30° angle have an edge roughness similar to horizontal lines, whereas image setting produced step-shaped lines.

We arrayed simple polygons to produce the photomasks illustrated in Figure 3. The resolution of the angles using photoplotting is poor for polygons as large as 25 μm: that is, the (for example) hexagonal shape is lost and the figure becomes

(20) Wu, H.; Odom, T. W.; Whitesides, G. M. *Adv. Mater.* **2002**, *14*, 1213−1216.
(21) Singhvi, R.; Kumar, A.; Lopez, G. P.; Stephanopoulos, G. N.; Wang, D. I. C.; Whitesides, G. M.; Ingber, D. E. *Science* **1994**, *264*, 696−698.
(22) Kumar, A.; Biebuyck, H. A.; Whitesides, G. M. *Langmuir* **1994**, *10*, 1498−1511.
(23) Chen, S. C.; Mrksich, M.; Huang, S.; Whitesides, G. M.; Ingber, D. E. *Science* **1997**, *276*, 1425−1428.
(24) Jiang, X.; Takayama, S.; Qian, X.; Ostuni, E.; Wu, H.; Bowden, N.; LeDuc, P.; Ingber, D. E.; Whitesides, G. M. *Langmuir* **2002**, *18*, 3273−3280.

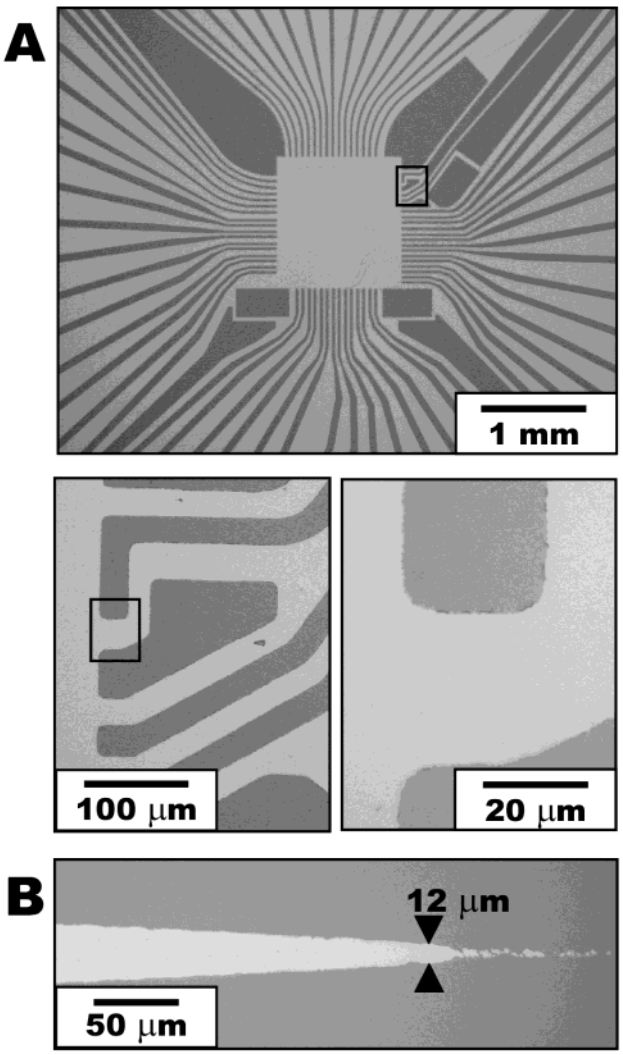

Figure 4. Optical microscopy pictures of metal pattern prepared by liftoff, using a photoplotted photomask. (A) Network of gold electrodes. For clarity, rectangles in the pictures outline the areas covered by the expanded views. (B) Triangle-shaped test structure, where the width of the palladium feature is well resolved down to 12 μm. Gold- or palladium-covered areas appear bright in the pictures.

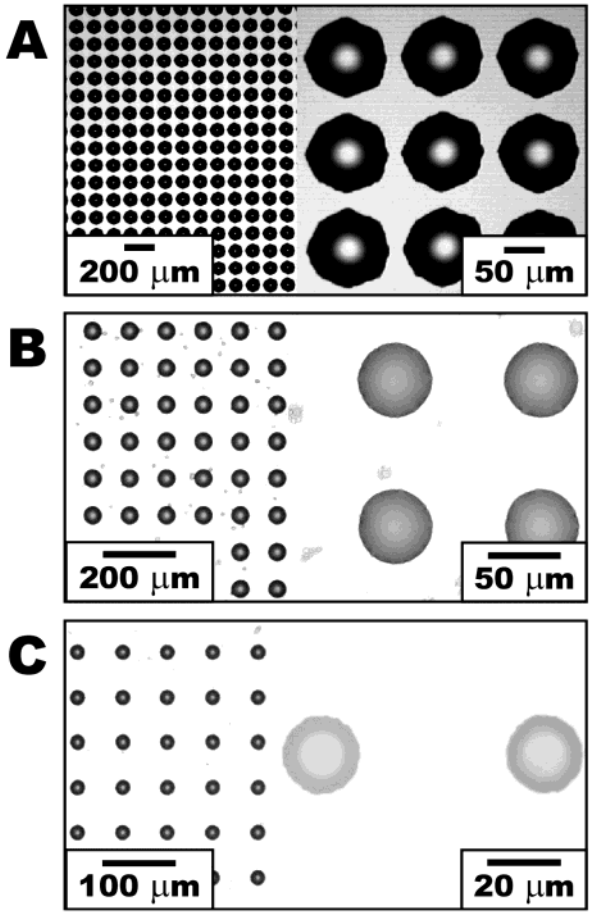

Figure 5. Optical microscopy pictures of microlens arrays: (A) 100-μm microlenses created using an image setting photomask, as previously described;[25] (B, C) 50- and 20-μm microlenses processed from photoplotted masks.

Table 1. Light Transmission (%) through Transparent Regions of Photomasks at Selected Wavelengths (Standard Deviations Calculated with $n = 3$)

wavelength (nm)	image setting	photoplotting	quartz
364 (i-line)	70 ± 1	75 ± 3	93 ± 1
405 (h-line)	74 ± 1	82 ± 1	93 ± 1
436 (g-line)	75 ± 1	85 ± 2	93 ± 1

circular. This problem was already identified for image setting, and since photoplotting is a technically improved version of image setting, we observed similar loss of resolution in photoplotted samples, but occurring at smaller dimensions.

Light transmission through the transparent areas of photomasks was measured at the wavelengths of three lines of mercury arc lamps (see Table 1). According to the average transmissions recorded at 364, 405, and 436 nm, the photoplotted films were 8% more transparent than the image setting ones. In the opaque areas, both types of transparency photomasks transmitted ~0.02% of incident light, which was similar to chromium masks (which transmitted ~0.01%). Microscope observation in the transparent areas of the photomasks revealed the presence of many dark spots. In the case of photoplotting, these spots were less numerous than for image setting photomasks and they appeared blurred because they were out of the plane of the features themselves (see, for example, Figure 1A and B).

Applications for Liftoff. We have transferred the pattern of the photomask into positive photoresist by photolithography. The resulting photoresist pattern was covered with a gold film to generate electrodes after a liftoff process. Figure 4A shows two expanded views of a network of gold electrodes covering an area of 1×1 cm^2. Electrodes that are 20 μm wide have smooth edges, and no short circuits between gold structures are noticeable by optical microscopy. We investigated the smallest dimension achievable by liftoff with a triangle-shaped pattern made of palladium. As seen in Figure 4B, the thickness of the feature decreases smoothly down to 12 μm; at smaller dimensions, the palladium structure is discontinuous.

Applications for Microlenses. The microlenses that we prepared previously using rapid prototyping were limited to a diameter of >100 μm,[25] because of the resolution of the photomasks available. Since photoplotting can generate circular shapes

(25) Wu, H. K.; Odom, T. W.; Whitesides, G. M. *J. Am. Chem. Soc.* **2002**, *124*, 7288−7289.

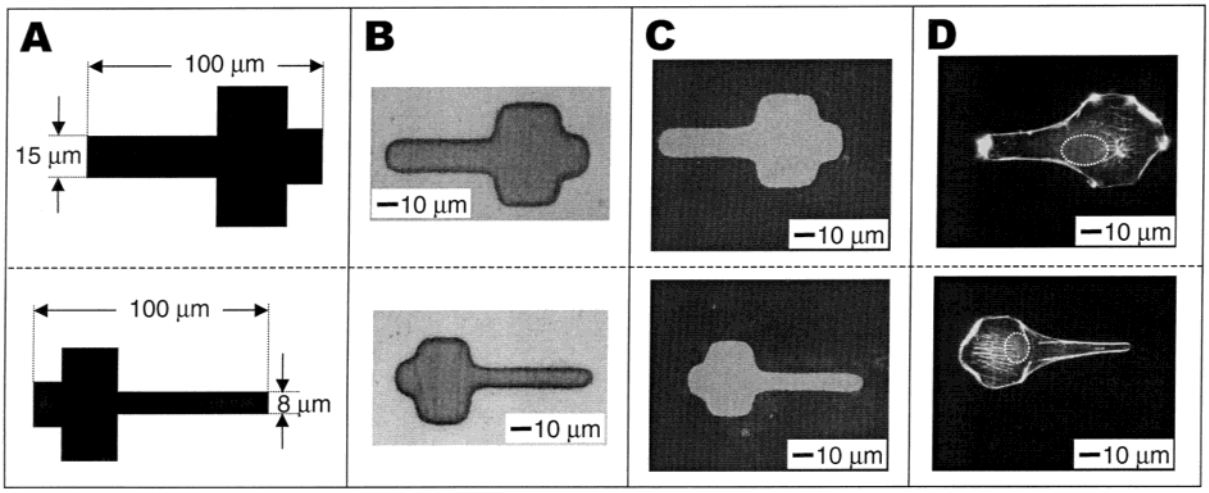

Figure 6. Patterning of cells on gold surfaces. (A) The shape of the features as drawn by CAD and (B) the corresponding photomask obtained by photoplotting. A μCP stamp was fabricated and used to generate a hydrophilic−hydrophobic SAM pattern on gold. (C) Fibronectin adsorbed on the hydrophobic patches of the pattern was visualized by fluorescence immunostaining. (D) Cells attached onto the fibronectin and spread over the available area defined by the pattern. For visualization, actin filaments of the cell were stained with 488-phalloidin and the nucleus was stained with DAPI (for clarity, the nucleus perimeter is outlined by a dotted line).

of higher quality than image setting, we have been able to prepare much smaller microlenses with no need for chromium masks. Figure 5 shows microlenses having 50- and 20-μm diameters. Their shape is more nearly circular than the 100-μm lenses prepared previously using image setting photomasks.

Application in Cell Biology. The study of single-cell behavior in artificial environments often requires the microfabrication of features as small as the single cells themselves. The lateral resolution achieved by photoplotting corresponds to the size of mammalian cells. In this application, we used a photomask to microfabricate a μCP stamp for the patterning of BCE cells on a gold substrate (see Figure 6). The pattern on the photomask covers an area equivalent to a fully spread BCE cell, with a lateral dimension of 8 μm. Using μCP, we printed hydrophobic attachment areas, where fibronectin was physisorbed and then stained by immunofluorescence. Figure 6C indicates that the attachment area defined by μCP is indistinguishable from the shape printed on the photomask. BCE cells incubated on the substrate attached to the physisorbed fibronectin and spread over the area of the printed region.

CONCLUSION

This paper demonstrates the technical improvement achieved by photoplotters in place of image setters for the generation of photomasks for use in soft lithography. The best lateral resolution achieved on a commercial photoplotted photomask can reach 8 μm. For most features, high resolution of perimeters is guaranteed down to 20-μm feature sizes, with an edge roughness of <1 μm. Below 20 μm, some types of patterns scale down better than others: in general, major losses of resolution occurring at the angles of polygons. In our experience, lines and curves give excellent results down to a width of 13 μm but become less reliable under that threshold value. The recent scientific literature[1−4,6−13] indicates that many research and industrial groups have adopted the use of printed photomasks instead of chromium masks for their work with structures larger than 25 μm. We have demonstrated that photoplotted photomasks extend the domain of application of soft lithography into the 8−25-μm range, with no significant increase in photomask price or delivery time.

ACKNOWLEDGMENT

This work was supported by a grant from NIH (GM65364). V.L. acknowledges a postdoctoral fellowship from the Swiss National Science Foundation. The authors thank R. Martino from CAD/ART Services, Inc. for providing valuable information about photoplotting and image setting techniques, and Prof D. E. Ingber (Children's Hospital and Harvard Medical School, Boston, MA) for kindly supplying the BCE cells.

Received for review December 18, 2002. Accepted March 7, 2003.

AC026441D